LOW LEVEL LONG WAVELENGTH LASER IRRADIATION EFFECTS ON CELL CYCLE PROGRESSION AND APOPTOSIS OF ENERGY RESTRICTED JURKAT T-CELLS

MIHAELA PISLEA, TEOFILA SEREMET*, GYÖNGYVÉR KATONA**, MAGDALENA MOCANU*, I.O. DOAGĂ***, E. RADU****, JUDIT HORVÁTH*****, E. TANOS*****, EVA KATONA*[#]*

*Department of Biophysics, **Department of Medical Biochemistry, ****Department of Molecular and Cellular Medicine, Medical Faculty, ***Department of Biophysics, Dentistry Faculty, "Carol Davila" University of Medicine and Pharmaceutics, Bucharest, Romania
*****LASEUROPA CO., Budapest, Hungary, [#]eva_katona@yahoo.com

Abstract. We investigated the effects of low power 680 nm far-red (FR) and 830 nm near-infrared (NIR) laser light on viability, survival/proliferation, apoptosis rate, and cell cycle progression of noninjured and energy restricted human acute T leukemic Jurkat cells. Data obtained both by microscopy and by flow cytometry demonstrated significant changes in the explored parameters. Energy restriction induced by blockade of oxidative phosphorylation with low concentrations of cyanide (1 mM NaCN) caused intoxication duration dependent viability and survival rate decrease, and apoptosis induction. NIR laser irradiation increased the percentage of live subpopulation in both non-injured and in cyanide intoxicated cell samples. FR laser light did not offer protection to non-injured Jurkat cells, but increased the percentage of live subpopulation in cyanide intoxicated samples. Cyanide intoxication caused G2/M stage blockade and apoptosis induction in an intoxication duration dependent manner. NIR and FR laser irradiation effects on human T leukemia lymphoblasts distribution in various cell cycle stages, as well as modulation of cyanide induced changes were dependent on cells state, duration of intoxication, and on irradiation dose. Low dose NIR irradiation promoted cell cycle progression, while at higher doses, an increase in percentage of cell subpopulations in G1 and G2 phases, and S-phase blockade with apoptosis promotion were observed in the NIR and FR irradiated non-injured samples, respectively. In the same conditions, with first irradiation applied early in the intoxication period, enhancement of the cyanide-induced G2 phase blockade and apoptosis induction occurred in FR irradiated samples, while NIR laser light appeared to cause S-phase cell accumulation in cyanide intoxicated samples.

Key words: AlGaInP/GaAs laser, cyanide-intoxication, human T leukemia lymphoblasts, photobiomodulation, cell viability.

INTRODUCTION

Low Level Laser Therapy (LLLT) uses long wavelength monochromatic light in the red (R) – far-red (FR) – near infrared (NIR) region to treat in a non-destructive and non-thermal fashion various soft-tissue and neurological conditions

Received February 2009.

ROMANIAN J. BIOPHYS., Vol. 19, No. 1, P. 1–18, BUCHAREST, 2009

[34, 62, 64]. Part of physiotherapy in most countries, LLLT proved to be very effective in healing infected, ischemic or hypoxic wounds [3, 18, 67], relieving pain [9, 10, 12, 16, 21, 54], reducing inflammation [3, 49, 55], mitigating mechanical injury caused or after-stroke tissue damage and neurological deficits [15, 44, 57]. Animal studies also demonstrated LLLT efficiency in overcoming intoxication by various toxins, in promotion of tissue repair and restoration of neural function [5, 6, 41, 45, 52]. Moreover, there is compelling evidence gathered in *in vitro* studies concerning low level R-IR laser irradiation beneficial effects at the cellular level: enhancement of cell adhesive properties, promotion of various cells survival / proliferation [2, 7, 14, 19, 23–25, 29, 33, 40, 42, 43, 51, 53, 54, 61, 63], of cellular protein synthesis [66, 72], modulation of cell signalling pathways and gene expression [1, 47, 48, 56, 68], reversal of various agents caused toxicity and restoration of function of intoxicated neural cells [65, 66]. A comparison of the action spectrum for laser photoirradiation induced stimulation of cellular proliferation, DNA/RNA synthesis, and of cell adhesion with the absorption spectra of potential photoacceptors allowed to suggest that cytochrome *c* oxidase is a primary photoacceptor of light in the R-NIR region [20–22, 31]. Reduction of this terminal enzyme of the respiratory chain with subsequent enhancement of the intramolecular electron transfer with stimulation of cellular energetics, are supposed to constitute the first steps in the photosignal transduction and amplification cascade [26–29, 32, 36]. Energy restriction induced by blockade of the mitochondrial respiratory chain, causing cytotoxic hypoxia through inhibition of the activity of cytochrome c oxidase, was proved to be deleterious in most cells, and prominently in differentiated ones [50]. Recent *in vitro* [33, 46, 65, 66] and *in vivo* [12] studies convincingly demonstrated the connection between the up-regulation of cytochrome c oxidase by R-NIR irradiation and protection of intoxicated retina or neurons [12, 13, 46, 65, 66], and HeLa cells [33]. Also existence of a signaling pathway between the mitochondria, the cellular membrane and the nucleus was hypothesized [30, 33], and lastly identified as retrograde mitochondrial signalling [35, 58]. Nevertheless, understanding of action mechanisms of R-NIR laser irradiation still remains fragmentary, and many details of molecular processes mediating the photosignal transduction and amplification cascade have to be elucidated in view of better design the therapeutic procedures and promotion of LLLT among branches of evidence based medicine.

This study was designed to investigate modulation by the 680 nm FR and the 830 nm NIR laser light, of the mild energy restriction caused effects occurring in human T leukemia lymphoblasts. Investigating impact of exposure to low concentrations of the potent inhibitor of cytochrome *c* oxidase sodium cyanide (NaCN) and/or to low doses (0.5–3 μJ/cell) of FR / NIR radiations, we report dose and exposure time dependent changes in cell death rates, survival/proliferation, apoptosis induction, and cell cycle progression of leukemic Jurkat cells, as follows:

(i) energy restriction induced by mild cyanide blockade of oxidative phosphorylation (NaCN, 1 mM) led to viability and survival rate decrease, G2/M stage blockade with apoptosis induction; (ii) cyanide effects were intoxication duration dependent; (iii) when applied after one day exposure, both FR and NIR laser irradiation increased the percentage live subpopulation in cyanide intoxicated samples; (iv) NIR irradiation induced live cell subpopulation increase even in control non-injured cell samples; (v) when applied within 8 h of toxin-exposure FR laser light induced S-phase blockade with apoptosis promotion in non-injured samples, while enhanced G2/M phase blockade induced by cyanide intoxication and promoted apoptosis of intoxicated cells; (vi) low dose (~1 μJ/cell) NIR irradiation of non-injured samples stimulated cell cycle progression, while in higher doses NIR caused increase in percentage cell subpopulations in G1 and G2 phases; (vii) progressing S-phase cell accumulation was observed in NIR irradiated cyanide intoxicated Jurkat cell samples.

MATERIALS AND METHODS

Chemicals, supplements and staining kits: Sterile DMSO, the standard RPMI 1640 culture medium (R6504, lyophilized powder, 1 vial/l), NaCN, the colorant Trypan Blue (TB, T8154, GM 960.81, 0.4% solution in 0.81% NaCl and 0.06% Na_2HPO_4), and the fluorophore Propidium Iodide (PI, P4170) were purchased from SIGMA CHEMICAL Co., Dulbecco's Phosphate Buffered Saline (PBS) 10× from BIOCHROME, while the supplements (FCS, foetal calf serum, EU tested, and antibiotics/glutamine) from GIBCO/INVITROGEN. The Annexine V-FITC (Ann.V-FITC) kit was from BECKMAN COULTER (IM 3546), while 7-AAD (559925, 0.5 mg/mL suspension in PBS with protein stabilizer and 0.09% sodium azide), and the PI/RNASE staining buffer (550825) were purchased from BD PHARMINGEN. All other chemicals were of the best research grade available.

Stock solutions: Ann.V binding buffer 10× was provided within the Ann.V-FITC kit. NaCN stock solution (20N) was prepared in 0.1 NaOH, while the PI stock solution (0.25 mg/mL) in PBS or Ann.V binding buffer.

Culture media: The standard RPMI 1640 medium was supplemented with 2 g/l sodium bicarbonate, 10% heat inactivated FCS, 100 U/mL penicillin, 100 μg/mL streptomycin, 2 mM L-glutamine, and pH was adjusted to 7.2 (complete medium, M). The serum deprived medium was prepared in the same way without adding FCS (M0 – M without FCS). The cyanide containing media were prepared from the complete medium (M), adding the appropriate quantity of NaCN stock solution (MX – M containing XmM NaCN).

Cell culture: The human acute T leukemic Jurkat cells were cultured in flasks or Petri dishes of variable surfaces, in humidified (80%) 5% CO_2 atmosphere at 37 ºC, in standard RPMI 1640 medium (M), and passaged every 2/3 days through dilution of cell suspensions with fresh media to a concentration of 6– 9×10^5 cells/mL.

Serum starvation: Cells were resuspended in M0 medium and incubated in the humidified (80%) 5% CO_2 atmosphere at 37°C for the indicated time periods (18–24 h) so as to establish metabolic quiescence.

Cyanide treatment: Cells were incubated in the humidified (80%) 5% CO_2 atmosphere at 37°C for various time periods in 1 mM NaCN containing media (M1), so as to establish hindrance of oxidative phosphorylation through cytochrome c oxidase inhibition caused blockade of the mitochondrial respiratory chain.

The irradiation sources were AlGaInP/GaAs based semiconductor lasers used in the medical practice, PHILIPS CQL806D and SONY SLD202-D3, with emission wavelengths and nominal powers of 680 nm/25 mW, and of 830 nm/50 mW, respectively.

Sample irradiation regimes and laser irradiation doses: Sample irradiation was performed in the laminar flow, with sources placed at a 10 cm height from the upper surface of cell suspensions, in 2–3 consecutive positions as to cover with the expanded laser speckle the whole surface of the suspension-containing Petri dishes rotating at a speed of 0.5 s^{-1}. Duration of treatment varied between 0–600 s, giving single incident doses equivalent with $(1–5)\times10^{12}$ photons/cell or ~ (0.2–1.5) μJ/cell. Irradiation regimes of once per day, or every second day with these single doses gave total irradiation doses of ~ (1–15) μJ/cell.

Cell viability and proliferation rate assessment through the TB exclusion method: After 16–22 h of serum starvation, cells in metabolic quiescence were resuspended in various media at a density of $0.6–0.9 \times 10^6$ cells/mL, distributed in 3.5–9 cm diameter Petri dishes, and further cultured for 18–96 h. At indicated time points cells in aliquots of 50 μL were stained with the TB colorant (final concentration ≤ 0.2%), visualized using a Zeiss Axiovert 25CFL or 40CFL inverted microscope. Live (TB excluding) and dead (TB stained) cells were counted in a Buerker-Tuerk hemocytometer.

Apoptosis detection: At different time point of exposure to various treatments (energy restriction / laser irradiation) cells were counted. 8×10^5 cells containing suspensions were pulse centrifuged at 4 ºC and resuspended in 1 mL ice-cold PBS. After a new pulse centrifugation washed cells were resuspended in 100 μL ice-cold Ann.V binding buffer (5×10^6 cells/mL). After adding 1 μL Ann.V-FITC and 2.5 μL 7-AAD (0.125 μg) or 5 μL PI stock solution (1.25 μg PI), samples were incubated 15 minutes in darkness, on ice. Following vigorous stirring of samples

completed with 400 μL Ann.V binding buffer, samples (~10^6 cells/mL) were kept in darkness on ice, and analyzed using a BD FACS Calibur flow cytometer within 2–3 h. Alternately cells were fixed in 2% paraformaldehyde (25 μL PFA 40% in 500 μL suspension) 30 minutes in darkness on ice, transferred in BD tubes and kept at 4 ºC until their analysis by flow cytometry within 2–3 days. Using for excitation the 488 nm line of the Ar ion laser, fluorescence intensities were measured at 520 nm (Ann.V-FITC), at $\lambda > 660$ nm (7-AAD) or at 617 nm (PI). Cells negative for Ann.V and 7-AAD/PI staining were considered alive, those stained by Ann.V-FITC, but not by 7-AAD/PI, early apoptotic (EA), while those stained both by Ann.V-FITC, and by 7-AAD/PI, late apoptotic or necrotic (LA+N) (Fig. 1a).

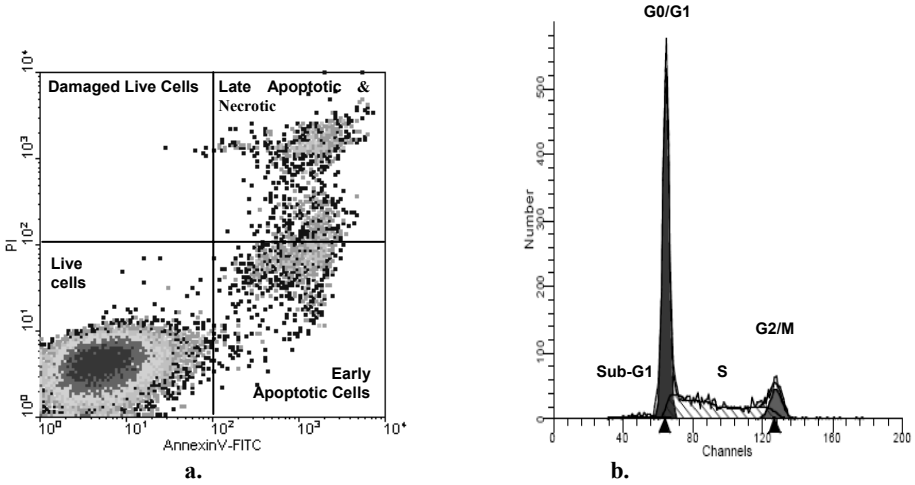

Fig. 1. Typical cell subpopulations identified in density plots and frequency histograms of data obtained by flow cytometric analysis of human T leukemic cells; a. Jurkat cell subpopulations identified in the 7-AAD(PI)/Ann.V-FITC density plots: live cells not stained either by FITC or by PI(7-AAD), early apoptotic (EA) cells with externalized phosphoserine (PS) stained by Ann.V-FITC, but plasma membranes impermeable to PI(7-AAD), late apoptotic (LA) and necrotic (N) cells with externalized PS and permeabilized plasma membranes stained by Ann.V-FITC and by PI(7-AAD), and damaged live cells not stained by Ann.V-FITC but stained by PI(7-AAD). Jurkat cells stained with Ann.V-FITC (IM3546 Beckman Coulter) and 7-AAD (559925 Pharmingen) or PI (SIGMA or Molecular Probes); fluorescence intensities measured by a BD FACS Calibur flow cytometer; data acquisition: CellQuest 3.0, data processing: WinMDI v.2.; b. Main cell cycle phases obtained by deconvolution of the DNA-content-frequency histogram: the G0/G1 and G2/M phase histogram peaks, the S-phase distribution, and the sub-G1 population considered as being constituted by apoptotic cells with fractional DNA content. Jurkat cells fixed with 70% EtOH and stained using a PI/RNAse kit (Pharmingen 550825). PI-fluorescence intensity proportional with cellular DNA content, measured by flow cytometry using a BD FACS Calibur instrument. Data acquisition: CellQuest 3.0, data processing: Modfit 2.0.

Cell Cycle Analysis: At appropriate time moments, samples of treated/untreated cells (~1.2×10^6) were pulse centrifuged and resuspended in 1 mL ice-cold PBS, pulse centrifuged and resuspended in 0.5 mL ice-cold PBS. Care was taken to meticulously disperse cells through repeated vigorous mixing as to avoid aggregate formation. Each thoroughly homogenized sample was introduced in 4.5 mL 0.70% (vol/vol) ethanol previously chilled at –24 ºC, ensuring comprehensive cell dispersing. Ethanol fixed cell samples, stable for weeks or even months, were kept at –24 ºC. On day of use samples were centrifuged at 200 g for 5 min, and decanting ethanol cells were resuspended in 5 mL PBS at room temperature for 1–2 min. Following a new centrifugation at 200 g for 5 min; cells were resuspended in PI/RNase staining buffer (0,5 mL/10^6 cells), and incubated 15 min at room temperature in darkness. Samples prepared were kept at 4 ºC in darkness until their analysis on a BD FACS Calibur flow cytometer with laser excitation at 488 nm using an emission 639 nm band pass filter to collect the red PI fluorescence intensity data CellQuest v.3.0 as acquisition software. The percentages of cells in the various phases of the cell cycle, namely, sub-G1, G0/G1, S, and G2/M, were assessed using the Modfit v.2.0 software (BD) (Fig.1b). Alternately, the freeware WinMDI 2.8 was used for row data analysis, and the histogram deconvolution software Cylchred for cell cycle distribution quantization.

Statistical Analysis: Viabilities and percentage and relative cell subpopulation sizes were obtained as means calculated from at least 3 independent assessments (standard deviation S.D. ≤ 15%). Unpaired analysis of data series obtained by measurements made on cells various time periods after their transfer in various modified media, irradiated and/or not irradiated, was performed by Student's t-test (two-tailed). *P*-values less than 0.05 were regarded as indicating statistical significance. Experiments were thrice performed, obtaining similar results. Percentages of cell populations in various cell cycle phases were calculated as averages of values given by the WinMDI software with marker defined histogram regions, and of values given by the deconvolution software Cylchred or Modfit 2.0, from measurements made on at least 2000 single cells. Standard deviations in individual samples were calculated/estimated from C.V. values supplied by the deconvolution programs.

RESULTS

Intoxication with 1 mM NaCN causes decrease in viability and proliferation of human T leukemic Jurkat cells, as seen 47 h after their resuspension in cyanide-containing medium. NIR laser light (830 nm, 0.9 μJ/cell) protects from cell viability decrease both the non-injured and the mildly cyanide-intoxicated human T leukemia lymphoblasts. FR laser light (680 nm, 1 μJ/cell) offers some protection to the cyanide-intoxicated cells, but not to the non-injured ones (Fig. 2).

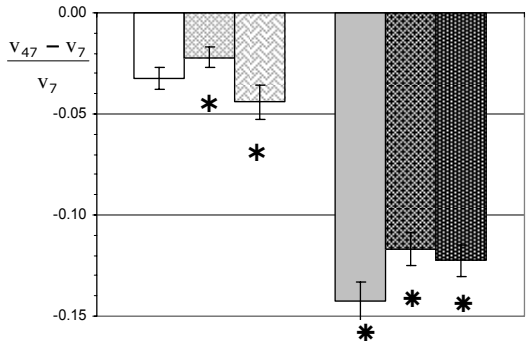

Fig. 2. Cyanide and laser irradiation effects on relative viability change of Jurkat cells 47 h after their resuspension in various media; Jurkat cells resuspended after 16 h of serum starvation (M0) in standard RPMI medium M (□) or in medium containing 1 mM NaCN (■, M1), some of them being irradiated with infrared (▨, ▨, NIR, 830 nm, 0.9 μJ/cell) and red (▨, ▩, FR, 680 nm, 1 μJ/cell) laser light respectively, 8 h after their resuspension; v_7 and v_{47} are cell viabilities determined 7 and 47 h after their resuspension in M/M1 respectively, by the TB exclusion method, counting TB excluding and TB stained cells in a Neubauer-Tuerk hemocytometer, using a Zeiss Axiovert 25CFL microscope; ✱ $p < 0.05$; ✱ $p < 0.01$.

At the same time counting of cells in a Neubauer-Tuerk hemacytometer 40 h after their irradiation does not reveal significant NIR induced changes in control Jurkat cells proliferation, while it discloses mild proliferation inhibition induced by FR. The same determinations show slight hindrance by NIR and promotion by FR irradiation of the cyanide intoxicated cells proliferation (Fig. 3).

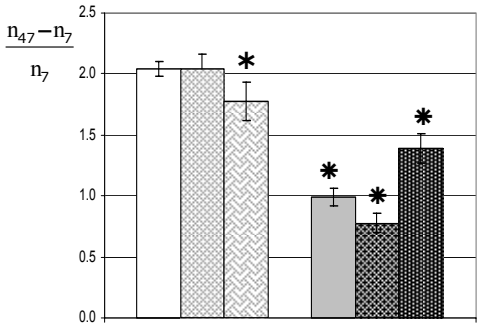

Fig. 3. Cyanide and laser irradiation effects on relative cell concentration increase in 40 h of Jurkat cells measured 47 h after their resuspension in various media; Jurkat cells resuspended after 16 h of serum starvation (M0) in standard RPMI medium Mc (□, M0M) or in medium containing 1 mM NaCN (■, M0M1), some of them being irradiated with infrared (▨, ▨, NIR, 830 nm, 0.9 μJ/cell) or red (▨, ▩, FR, 680 nm, 1 μJ/cell) laser light respectively, 8 h after their resuspension; n_{47} and n_7 are the cell numbers in unit volume, counted in a Neubauer-Tuerk hemacytometer 47 and 7 h after cells resuspension in media, using a Zeiss Axiovert 25CFL microscope; ✱ $p < 0.05$; ✱ $p < 0.01$.

Flow cytometric assessment of percentage subpopulations of live, dying (early apoptotic, EA) and dead (late apoptotic and necrotic, LA+N) cells discloses significant photobiomodulation of Jurkat cells survival. Hindrance of oxidative phosphorylation through blockade of mitochondrial respiratory chain with cyanide (1 mM NaCN, 24–48 h, M0M1) results in decrease of live cell subpopulation with apoptosis induction (Figs. 4 and 5).

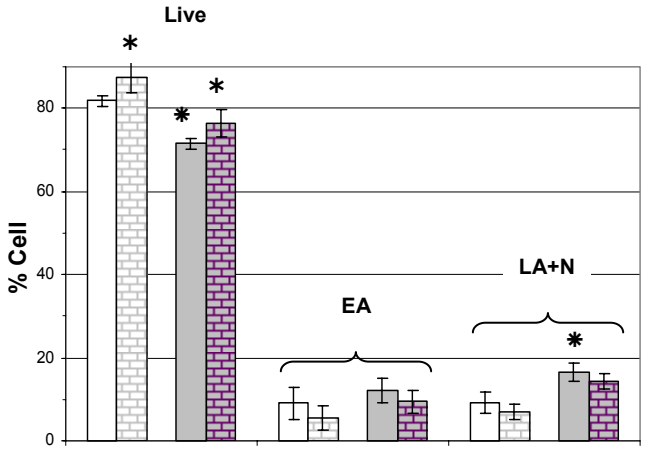

Fig. 4. NIR laser irradiation effects on live, dying and dead cell subpopulations sizes, seen in Ann.V-FITC and PI stained control and cyanide-exposed human T leukemic cell cultures; Jurkat cells stained with Ann.V-FITC and PI 24 h after serum starved (23 h) cells resuspension in standard RPMI medium (□, M0M) and in medium containing 1 mM NaCN (▩, M0M1) respectively. Control and cyanide-treated cells and cells irradiated with near-infrared (NIR, 830 nm, 0.5 μJ/cell) laser light (▦, ▩), 2 h after their resuspension. Flow cytometric data obtained using a BD FACS Calibur instrument with CellQuest 3.0 and WinMDI 2.8 as acquisition and analysis software respectively; ✱ statistically significant difference as compared to control ($p < 0.05$), ❋ statistically significant difference as compared to control ($p < 0.01$).

NIR laser irradiation (830 nm, 0.5 μJ/cell) increases in 22 h the live cells subpopulations in both control and cyanide intoxicated (M0M1) Jurkat cells (Fig. 4). FR laser light (680 nm, 0.9 μJ/cell) apparently does not affect sizes of percentage subpopulations of live, dying and dead cells in control samples, as determined 24 h after irradiation of non-injured Jurkat cells. In the same conditions FR laser irradiation results in increase of live cell subpopulation and decrease of both EA and (LA+N) subpopulations sizes in cyanide intoxicated samples (Fig. 5).

Flow cytometric follow-up of cell cycle progression 16 h after irradiation does not reveal substantial changes induced by NIR (0.9 μJ/cell) or FR (1 μJ/cell) laser light in non-injured human T leukemia lymphoblasts distribution in various cell cycle stages, except for a slight decrease in the rate of apoptotic cells, and mild stimulation of cell cycle progression by the NIR laser light (Fig. 6).

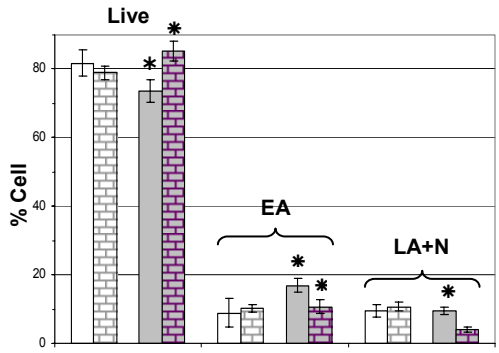

Fig.5. FR laser irradiation effects on live, dying and dead cell subpopulations sizes, seen in Ann.V-FITC and 7-AAD stained control and cyanide-exposed human T leukemic cell cultures; Jurkat cells stained with Ann.V-FITC and 7-AAD 46 h after serum starved (16 h) cells resuspension in standard RPMI medium (□, M0M) and in medium containing 1 mM NaCN (▢, M0M1) respectively. Control and cyanide-treated cells and cells irradiated with far-red (FR, 680 nm, 0.9 μJ/cell) laser light (▢, ▢), 22 h after their resuspension. Flow cytometric data obtained using a BD FACS Calibur instrument with CellQuest 3.0 and WinMDI 2.8 as acquisition and analysis softwares respectively; ✱ statistically significant difference as compared to control ($p < 0.05$); ✱ statistically significant difference as compared to control ($p < 0.01$).

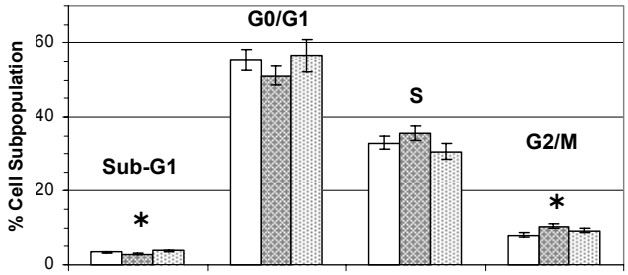

Fig. 6. Photobiomodulation of percentage distribution of Jurkat cells in cell cycle stages, seen 24 h after cells resuspension in complete medium, and 16 h after their irradiation; Jurkat cells resuspended after 16 h of serum starvation (M0) in standard RPMI medium with 10% FCS (□, Mc), some of them 8 h after their resuspension being irradiated with infrared (▩, NIR, 830 nm, 0.86 μJ/cell) and red (▩, FR, 680 nm, 1.05 μJ/cell) laser light respectively. The sub-G1 population is constituted of apoptotic cells, while G0/G1, S and G2/M are cell populations in the respective cell cycle stages. Bars represent ±S.D. calculated (G1, G2) / estimated (S, subG1) from the C.V. supplied by the deconvolution program Cylchred following analysis of cell cytometric measurements on 7540, 10060 and 6282 cells respectively. Measurements made on cells fixed in 70% EtOH, and stained using a PI/RNAse Kit (Pharmingen 550825). Data collected on a Becton-Dickinson FACS Calibur flow cytometer. Software used for data analysis and deconvolution of DNA content histograms: WinMDI 2.8 and Cylchred. ✱ statistically significant difference as compared to control ($p < 0.05$).

Changes become important at double doses, as it can be seen 1 h after the second irradiation (44 h after the first one). Increase in percentage cell subpopulations in both G1 and G2 phases in NIR irradiated samples, and S-phase

blockade with apoptosis promotion in FR irradiated cells are observed in these conditions (Fig. 7).

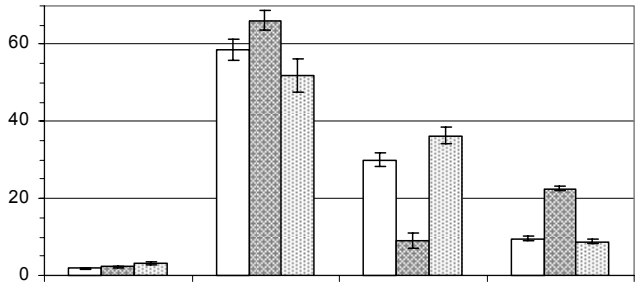

Fig. 7. Photobiomodulation of percentage distribution of Jurkat cells in cell cycle stages, seen 53 h after cells resuspension in complete medium, and 1 h after their second irradiation; Jurkat cells resuspended after 16 h of serum starvation (M0) in standard RPMI medium with 10% FCS (□, M), some of them being twice irradiated (8 h and 52 h after their resuspension) with infrared (▩, NIR, 830 nm, 1.8 μJ/cell) and red (▨, FR, 680 nm, 2 μJ/cell) laser light respectively. The sub-G1 population is constituted of apoptotic cells, while G0/G1, S and G2/M are cell populations in the respective cell cycle stages. Bars represent ±S.D. calculated (G1, G2) / estimated (S, subG1) from the C.V. supplied by the deconvolution program Cylchred following analysis of flow cytometric measurements on 2325, 255 and 7635 cells respectively. Measurements made on cells fixed in 70% EtOH, and stained using a PI/RNAse Kit (Pharmingen 550825). Data collected on a Becton-Dickinson FACS Calibur flow cytometer. Softwares used for data analysis and deconvolution of DNA content histograms: WinMDI 2.8 and Cylchred; ✱ statistically significant difference as compared to control ($p < 0.05$); ✱ statistically significant difference as compared to control ($p < 0.01$).

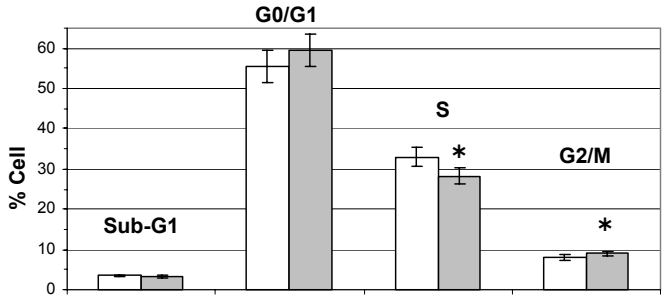

Fig. 8. Cyanide effects on percentage distribution of Jurkat cells in cell cycle stages, seen 24 h after cells resuspension in 1 mM NaCN containing medium; Jurkat cells resuspended after 16 h of serum starvation (M0) in standard RPMI medium with 10% FCS (Mc), containing 1 mM NaCN. The sub-G1 population is constituted of apoptotic cells, while G0/G1, S and G2/M are cell populations in the respective cell cycle stages. Bars represent ±S.D. calculated (G1, G2) / estimated (S, subG1) from the C.V. supplied by the deconvolution program Cylchred following analysis of cell cytometric measurements on 7680 and 10274 cells respectively. Measurements made on cells fixed in 70% EtOH, and stained using a PI/RNAse Kit (Pharmingen 550825). Data collected on a Becton-Dickinson FACS Calibur flow cytometer. Softwares used for data analysis and deconvolution of DNA content histograms: WinMDI 2.8 and Cylchred; ✱ statistically significant difference as compared to control ($p < 0.05$).

1 mM NaCN induced blockade of the respiratory chain results in changes of Jurkat cells distribution in main cell cycle stages in 24 h, with decrease in the cell subpopulation in the S phase and increase of that in the G2/M phase. At this time moment apoptosis induction is not manifest (Fig. 8).

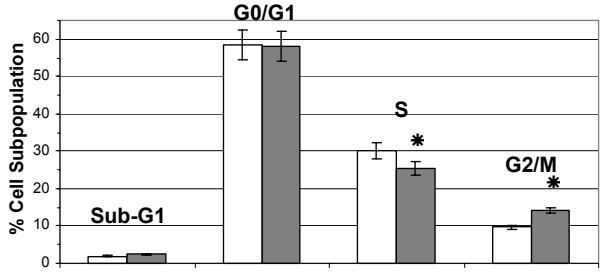

Fig. 9. Cyanide effects on percentage distribution of Jurkat cells in cell cycle stages, seen 53 h after cells resuspension in 1 mM NaCN containing medium; Jurkat cells resuspended after 16 h of serum starvation (M0) in standard RPMI medium with 10% FCS (Mc), containing 1 mM NaCN. The sub-G1 population is constituted of apoptotic cells, while G0/G1, S and G2/M are cell populations in the respective cell cycle stages. Bars represent standard deviations calculated in cell cytometric measurements on 2325 and 975 cells respectively. Measurements made on cells fixed in 70% EtOH, and stained using a PI/RNAse Kit (Pharmingen 550825). Data collected on a Becton-Dickinson FACS Calibur flow cytometer. Softwares used for data analysis and deconvolution of DNA content histograms: WinMDI 2.8 and Cylchred; ✱ statistically significant difference as compared to control ($p < 0.05$); ✱ statistically significant difference as compared to control ($p < 0.01$).

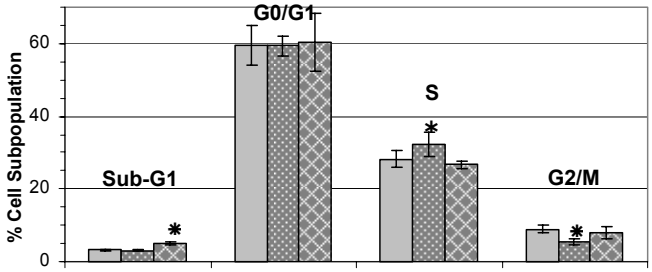

Fig. 10. Photobiomodulation of cyanide effects on percentage distribution of Jurkat cells in cell cycle stages, seen 24 h after their resuspension in 1 mM NaCN containing medium; Jurkat cells resuspended after 16 h of serum starvation (M0) in standard RPMI medium with 10% FCS, and 1 mM NaCN (▢, M1), some of them being irradiated with infrared (▩, NIR, 830 nm, 0.86 μJ/cell) and red (▨, FR, 680 nm, 1.05 μJ/cell) laser light respectively, 8 h after their resuspension. The sub-G1 population is constituted of apoptotic cells, while G0/G1, S and G2/M are cell populations in the respective cell cycle stages. Bars represent ± S.D. calculated (G1, G2) / estimated (S, subG1) from the C.V. supplied by the deconvolution program Cylchred following analysis of cell cytometric measurements on 10274, 7020 and 5130 cells respectively. Measurements made on cells fixed in 70% EtOH, and stained using a PI/RNAse Kit (Pharmingen, 550825). Data collected on a Becton-Dickinson FACS Calibur flow cytometer. Softwares used for data analysis and deconvolution of DNA content histograms: WinMDI 2.8 and Cylchred; ✱ statistically significant difference as compared to control ($p < 0.05$); ✱ statistically significant difference as compared to control ($p < 0.01$).

Following 53 h exposure, the G2/M stage blockade and apoptosis induction are clearly recognizable (Fig. 9). S-phase cell accumulation induced by NIR irradiation and apoptosis induction by FR irradiation is observed in 16 h in cyanide-intoxicated (24 h exposure) T leukemia lymphoblasts (Fig. 10).

Both changes become more substantial after 53 h exposure and additional irradiation (1.8 and 2 μJ/cell total dose, respectively). Assessing cell cycle progression 1 h after the second irradiation (45 h after the first one), intensification of the NIR-induced S-phase cell accumulation as well as clear enhancement of the cyanide-induced G2 phase blockade and apoptosis induction under the influence of the FR laser light are evident. No enhancement by NIR of the cyanide-induced apoptosis induction is apparent in the given conditions (Fig. 11).

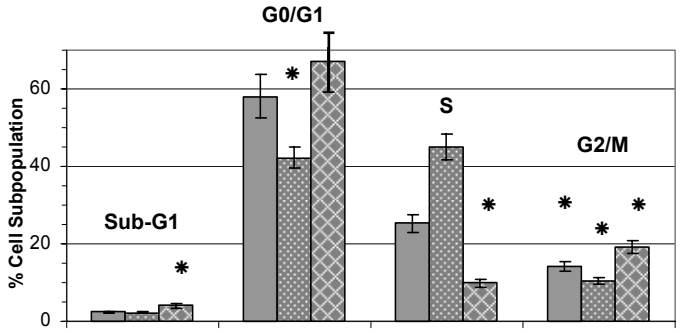

Fig. 11. Photobiomodulation of cyanide effects on percentage distribution of Jurkat cells in cell cycle stages, seen 53 h after their resuspension in 1 mM NaCN containing medium and 1 h after their second irradiation; Jurkat cells resuspended after 16 h of serum starvation (M0) in standard RPMI medium with 10% FCS, and 1 mM NaCN (□, M1), some of them being twice irradiated with infrared (▩, NIR, 830 nm, 1.8 μJ/cell) and red (▩, FR, 680 nm, 2 μJ/cell) laser light respectively, 8 h and 52 h after their resuspension. The sub-G1 population is constituted of apoptotic cells, while G0/G1, S and G2/M are cell populations in the respective cell cycle stages. Bars represent ± S.D. calculated (G1, G2) / estimated (S, subG1) from the C.V. supplied by the deconvolution program Cylchred following analysis of cell cytometric measurements on 975, 1755 and 240 cells respectively. Measurements made on cells fixed in 70% EtOH, and stained using a PI/RNAse Kit (Pharmingen, 550825). Data collected on a Becton-Dickinson FACS Calibur flow cytometer. Softwares used for data analysis and deconvolution of DNA content histograms: WinMDI 2.8 and Cylchred;
✱ statistically significant difference as compared to control ($p < 0.01$).

DISCUSSION AND CONCLUSIONS

High quality investigations undertaken in the past 4 decades convincingly indicated the endogenous mitochondrial enzyme, cytochrome c oxidase, as the most important biological photoacceptor in the R-FR-NIR range [20–22, 26–28, 36, 66, recently reviewed in 34]. The $Cu_A \rightarrow$ [heme a] $\Rightarrow$ [heme a_3-Cu_B] $\rightarrow O_2$ electron transfer within cytochrome c oxidase proceeds on a microsecond time

scale (→) between Cu_A and [heme a] and between the catalytic center [heme a_3-Cu_B] and dioxygen. The only rate-limiting stage appears to be the internal electron transfer occurring on a millisecond time scale between [heme a] and the [heme a_3-Cu_B] pair. The variability of the electron transfer rate at the interheme point is believed to be a controlling factor in the enzyme turnover [4, 16]. One could speculate that R-FR-NIR irradiation, increasing the availability of electrons, intensifies exactly this electron transfer stage [33], and intensification under exposure to visible light of electron transfer activity in an isolated cytochrome c oxidase molecule inhibited by low concentrations of potassium cyanide, was indeed demonstrated [cited in 33].

R-FR-IR irradiation engendered restoration or protection of cytochrome c oxidase activity in various cells – more important in highly oxidative ones – was extensively demonstrated [reviewed in 33–35] no matter whether function loss was consequence of direct action or of indirect downregulation [66]. Therefore, absorption of laser light by the copper chromophores of cytochrome c oxidase, with subsequent enzyme reduction, stimulation of intramolecular electron transfer and of cellular energetics, are generally accepted as most important primary mechanisms mediating photobiomodulation in the R-FR-IR range [34, 66]. As concerns further steps of the photosignal transduction and amplification chain, their characterization – yet far from being complete – is in full progress [reviewed in 34–35]. In this retrograde – mitochondrial to nucleus – signaling, changes occurring in cell membrane properties, and in cell cytoplasm characteristics sustaining pathways leading to cell survival, proliferation or death, constitute important intermediary mechanisms [35].

We previously reported significant changes induced by the 680 nm FR and the 830 nm NIR laser irradiation in the plasma membrane properties of human blood cells [37–39], and in Jurkat cells mitochondrial membrane state [10] underlining metabolic modulation of the observed changes, as well as changes occurring following various protocols of energy/nutrient restriction. We also disclosed significant photobiomodulation of quercetin cytotoxicity in human T leukemia lymphoblasts [59].

In the present study we focused on disclosure of photobiomodulation of mild cyanide intoxication effects in human T leukemic cells. Our findings are consistent with the hypothesis that cyanide intoxication caused blockade of oxidative phosphorylation results in progressing viability and survival rate decrease. Increasing G2/M phase cell cycle blockade with apoptosis induction appears to constitute the underlying mechanism. However, the revealed changes are moderate, in accordance with the fact that in leukemic cells glycolysis contribution to cellular energetics is substantial. FR laser light induced S-phase blockade with apoptosis promotion in non-injured T leukemic cell samples. Low dose (~1 μJ/cell) NIR irradiation of non-injured Jurkat cells induced live cell subpopulation increase and stimulated cell cycle progression, as seen 16 h after sample irradiation. In higher

doses (2 μJ/cell) NIR caused increase in percentage cell subpopulations in G1 and G2 phases, without apparent apoptosis promotion, as assessed 1 h after the second irradiation. When applied after one day cyanide exposure, both FR and NIR laser irradiation increased the percentage live subpopulation in intoxicated samples. FR irradiation, applied in early phases of the intoxication period, caused progressing dose-dependent enhancement of the cyanide induced G2/M phase blockade with apoptosis induction. In same conditions NIR induced S-phase accumulation in cyanide intoxicated Jurkat cell samples.

In sum, significant changes in viability, survival/proliferation, cell cycle progression and apoptosis induction were observed in Jurkat cells under the influence both of cyanide intoxication caused energy restriction and of FR / NIR laser irradiation. The revealed changes are clearly dependent on energy restriction caused stress duration, radiation wavelength and irradiation dose. Further investigations into this issue are underway in our laboratories.

Moreover, we confirm that [17] an additional parameter – the time lag elapsed between the last irradiation of the sample and the time moment of effect assessment – should be compulsorily indicated, when LLLT effects are reported.

Acknowledgments: Partial financial support of the Ministry of Education and Research of Romania (Grant CNCSIS 924/2006) is gratefully acknowledged.

REFERENCES

1. AIHARA, N., M. YAMAGUCHI, K. KASAI, Low-energy irradiation stimulates formation of osteoblast-like cells via RANK expression in vitro, *Laser Med. Sci.*, 2006, **21**, 24–33.
2. ALMEIDA-LOPES, L. *et al.*, Comparison of the low level laser therapy effects on cultured human gingival fibroblasts proliferation using different irradiance and same fluence, *Lasers Surg. Med.*, 2001, **29**(2), 179–184.
3. ARORA, H, K.M. PAI, A. MAIYA, M.S. VIDYASAGAR, A. RAJEEV, Efficacy of He-Ne Laser in the prevention and treatment of radiotherapy-induced oral mucositis in oral cancer patients, *Oral Surg. Oral Med. Oral Pathol. Oral Radiol. Endod*., 2008, **105**, 180–6.
4. BRUNORI, M., A. GIUFFRE, P. SARTI, Cytochrome c oxidase, ligands and electrons, *J. Inorg. Biochem*., 2005, **99**, 324–336.
5. BYRNES, K.R. *et al*., Cellular invasion following spinal cord lesion and low power laser irradiation, *Lasers Surg. Med*., 2002, **S14**, 11–16.
6. CASTRO-E-SILVA, T., O. CASTRO-E-SILVA, C. KURACHI, J. FERREIRA, S. ZUCOLOTO, V.S. BAGNATO, The use of light-emitting diodes to stimulate mitochondrial function and liver regeneration of partially hepatectomized rats, *Braz. J. Med. Biol. Res*., 2007, **40**, 1065–9.
7. CHENG, L., T.C. LIU, J.-Q. CHI, Y. LI, H. JIN, Photobiomodulation on the proliferation and collagen synthesis of normal human skin fibroblast cells, *Proc. SPIE*, 2006, **6026,** 63–72.
8. CHOW, R.T., G.Z. HELLER, L. BARNSLEY, The effect of 300 mW, 830 nm laser on chronic neck pain: a double-blind, randomized, placebo-controlled study, *Pain*, 2006, **124**, 201–210.
9. DJAVID, G.E., R. MEHRDAD, M. GHASEMI, H. HASAN-ZADEH, A. SOTOODEH-MANESH, G. POURYAGHOUB, In chronic low back pain, low level laser therapy combined with exercise is more beneficial than exercise alone in long term: a randomized trial, *Aust. J. Physiother.*, **53**, 2007, 155–160.

10. DOAGA, I.O., E. RADU, GY. KATONA, T. SEREMET, M. DUMITRESCU, S. RADESI, M. PISLEA, J. HORVÁTH, E. TANOS, L. KATONA, E. KATONA, Low level long wavelength laser irradiation effects on human T leukemic lymphoblasts mitochondrial membrane potential, *Rom. J. Biophys.*, 2008, **18**(1), 1–17.
11. DUNDAR, U., D. EVCIK, F. SAMLI, H. PUSAK, V. KAVUNCU, The effect of gallium arsenide aluminum laser therapy in the management of cervical myofascial pain syndrome: a double blind, placebo-controlled study, *Clin. Rheumatol*., 2007, **26**, 930–4.
12. EELLS, J.T., M.M. HENRY, P. SUMMERFELT, M.T.T. WONG-RILEY, E.V. BUCHMANN, M. KANE, N.T. WHELAN, H.T. WHELAN, Therapeutic photobiomodulation for methanol-induced retinal toxicity, *Proc. Natl. Acad. Sci. USA*, 2003, **100**, 3439–3444.
13. EELLS, J., M.T. WONG-RILEY, J. VERHOEVE, M. HENRY, E.V. BUCHMAN, M.P. KANE, L.J. GOULD, R. DAS, M. JETT, B.D. HODGSON, D. MARGOLIS, H.T. WHELAN, Mitochondrial signal introduction in accelerated wound and retinal healing by near-infrared light therapy, *Mitochondrion*, 2004, **4**, 559–567.
14. EL BATANOUNY, M., S. KORRAA, O. FEKRY, Mitogenic potential inducible by He:Ne laser in human lymphocytes in vitro, *J. Photochem. Photobiol. B: Biology*, 2002, **68**(1), 1–7.
15. ENWEMEKA, C.S., J.C. PARKER, D.S. DOWDY, E.E. HARKNESS, L.E. SANFORD, L.D. WOODRUFF, The efficacy of low power lasers in tissue repair and pain control: a meta-analysis study, *Photomed. Laser Surg*., 2004, **22**, 323–329.
16. FARVER, O., O. EINARSDOTTIR, I. PECHT, Electron transfer rates and equilibrium within cytochrome c oxidase, *Eur. J. Biochem.*, 2000, **267**, 950–954.
17. HAWKINS, D., H. ABRAHAMSE, Time-dependent responses of wounded human skin fibroblasts following phototherapy, *J. Photochem. Photobiol. B: Biology*, 2007, **88**,147–155.
18. HAWKINS, D., H. ABRAHAMSE, Phototherapy – a treatment modality for wound healing and pain relief, *Afr. J. Biomed. Res.*, 2007, **10**, 99–109.
19. HU, W.-P., J.J. WANG, C.-L. YU, C.-C.E. LAN, G.S. CHEN, H.-S. YU, He-Ne laser irradiation stimulates cell proliferation through photostimulatory effects in mitochondria, *J. Invest. Dermatol*., 2007, **127**, 2048–57.
20. KARU, T.I., *Photobiology of Low-Power Laser Therapy*, Harwood Academic, London, 1989.
21. KARU, T., *The Science of Low Power Laser Therapy*, Gordon and Breach Science Publishers, London, 1998
22. KARU, T., Mechanisms of low-power laser light action on cellular level, in: *Lasers in Medicine and Dentistry,* Z. Simunovic (Ed.), Vitgraf, Rijeka, 2000, Ch.IV, pp. 97–125.
23. KARU, T.I., L.V. PYATIBRAT, G.S. KALENDO, Cell attachment modulation by radiation from a pulsed semiconductor light diode (lambda = 820 nm) and various chemicals, *Lasers Surg. Med.*, 2001, **28**, 227–236.
24. KARU, T.I., L.V. PYATIBRAT, G.S. KALENDO, Studies into the action specifics of a pulsed GaAlAs laser (λ = 820 nm) on a cell culture. I. Reduction of the intracellular ATP concentration: dependence on initial ATP amount, *Lasers Life Sci*., 2001, **9**, 203–210.
25. KARU, T.I., L.V. PYATIBRAT, G.S. KALENDO, Studies into the action specifics of a pulsed GaAlAs laser (λ = 820 nm) on a cell culture. II. Enhancement of the adhesive properties of cellular membranes: dependence on the dark period between pulses, *Lasers Life Sci*., 2001, **9**, 211–217.
26. KARU, T.I., Low-power laser effects, in: *Lasers in Medicine*, R. Waynant (Ed.), Boca Raton, CRC Press, 2002, pp. 171–209.
27. KARU, T.I., Low power laser therapy, in: *Biomedical Photonics Handbook*, Tuan Vo-Dinh (Ed.), CRC Press, Boca Raton 2003, Ch. 48, pp. 48-1–48-25.
28. KARU, T.I., Cellular mechanism of low power laser therapy: new questions, in: *Lasers in Medicine and Dentistry*, Vol. 3., Z. Simunovic (Ed.), Vitgraf, Rijeka, 2003, Ch. IV., pp. 79–100.
29. KARU, T.I., L.V. PYATIBRAT, G.S. KALENDO, Photobiological modulation of cell attachment via cytochrome c oxidase, *Photochem. Photobiol. Sci*., 2004, **3**, 211–216.

30. KARU, T.I., L.V. PYATIBRAT, N.I. AFANASYEVA, A novel mitochondrial signaling pathway activated by visible-to-near infrared radiation, *Photochem. Photobiol.*, 2004, **80**, 366–372.
31. KARU, T., S.F. KOLYAKOV, Exact action spectra for cellular responses relevant to phototherapy, *Photomed. Laser Surg*., 2005, **23**, 355–361.
32. KARU, T, L.V. PYATIBRAT, S.F. KOLYAKOV, N.I. AFANASYEVA, Absorption measurements of a cell monolayer relevant to phototherapy: Reduction of cytochrome c oxidase under near IR radiation, *J. Photochem. Photobiol. B: Biology*, 2005, **81**, 983–106.
33. KARU, T., Attachement of cells can be increased by monochromatic light in the red-to-near-IR region: a novel mitochondrial signaling pathway, in: *Photodynamic Therapy at the Cellular Level*, A.B.Uzdensky (Ed.), Research Signpost, Kerala, India, 2007, pp. 1–39.
34. KARU, T., *Ten lectures on basic science of laser phototherapy*, Prima Books AB, Grangesberg, Sweden, 2007.
35. KARU, T.I., Mitochondrial signaling in mammalian cells activated by red and near-IR radiation, *Photochem. Photobiol.*, 2008, **84**, 1091–9.
36. KARU, T.I., L.V. PYATIBRAT, S.F. KOLYAKOV, N.I. AFANASYEVA, Absorption measurements of cell monolayers relevant to laser phototherapy: reduction or oxidation of cytochrome c oxidase under laser radiation at 632.8 nm, *Photomed. Laser Surg.*, 2008, **26**(6), 593–9.
37. KATONA, E., GY. KATONA, A. CĂPLĂNUŞI, I.O. DOAGĂ, D. IONESCU, R. MATEI, J. HORVÁTH, E. TRUŢIA, E. TANOS, L. KATONA, Low power red laser irradiation effects, as seen in metabolically intact and impaired human blood cells, *Rom. J. Biophys*., 2003, **13**(1–4), 1–16.
38. KATONA, E., GY. KATONA, I.O. DOAGĂ, T. ŞEREMET, M. DUMITRESCU, S. RADESI, R. MATEI, J. HORVÁTH, E. TANOS, L. KATONA, Membrane effects of low level infrared laser irradiation, as seen in metabolically intact and impaired human blood cells, *Rom. J. Biophys*., 2004, **14**(1–4), 99–108.
39. KATONA, E., GY. KATONA, I.O. DOAGĂ, D. IONESCU, R. MATEI, J. HORVÁTH, E. TANOS, L. KATONA, Multiple low level laser irradiation effects on human peripheral blood lymphocytes and platelets, revealed by fluorimetric techniques, *Rom. J. Biophys*., 2006, **16**(4), 221–228.
40. KHADRA, M., S.P. LYNGSTADAAS, H.R. HAANÆS, K. MUSTAFA, Effect of laser therapy on attachment, proliferation and differentiation of human osteoblast-like cells cultured on titanium implant material, *Biomaterials*, 2005, **26**(17), 3503–9.
41. KOJI, M., A. AKIRA, A.A. TAKASAKI, A. KINOSHITA, C. HAYASHI, S. ODA, I. ISHIKAWA, Periodontal tissue healing following flap surgery using an Er:YAG laser in dogs, *Lasers Surg. Med*., 2006, **38**(4), 314–324.
42. KREISLER, M., A.B. CHRISTOFFERS, B. WILLERSHAUSEN, B. D'HOEDT, Effect of low-level GaAlAs laser irradiation on the proliferation rate of human periodontal ligament fibroblasts: an *in vitro* study, *J. Clin. Periodontol*., 2003, **30**(4), 353–8.
43. LAGE, C., P.C.N. TEIXEIRA, A.C. LEITAO, Non-coherent visible and infrared radiation increase survival to UV (354 nm) in Echerichia coli K 12, *J. Photochem. Photobiol. B: Biology*, 2000, **54**, 155–161.
44. LAMPL, Y., J.A. ZIVIN, M. FISHER, R. LEW, L. WELIN, B DAHLOF, P. BORENSTEIN, B. ANDERSSON, J. PEREZ, C. CAPARO, S. ILIC, U. ORON, Infrared laser therapy for ischemic stroke: a new treatment strategy. results of the neurothera effectiveness and safety trial-1 (NEST-1), *Stroke*, 2007, **38**, 1843–9.
45. LAPCHAK, P.A., K.F. SALGADO, C.H. CHAO, J.A. ZIVIN, Transcranial near-infrared light therapy improves motor function following embolic strokes in rabbits: an extended therapeutic window study using continuous and pulse frequency delivery modes, *Neurosci.*, 2007, **140**, 339–49.
46. LIANG, H.L., H.T. WHELAN, J.T. EELLS, H. MENG, E. BUCHMANN, A. LERCH-GAGGL, M. WONG-RILEY, Photobiomodulation partially rescues visual cortical neurons from cyanide-induced apoptosis, *Neurosci.*, 2006, **139**, 639–649.

47. LUBART, R., M. EICHLER, R. LAVI, H. FRIEDMAN, A. SHAINBERG, Low-energy laser irradiation promotes cellular redox activity, *Photomed. Laser Surg*., 2005, **23**, 3–9.
48. MAFRA DE LIMA, F., Low level laser therapy (LLLT): Attenuation of cholinergic hyperreactivity, β2-adrenergic hyporesponsiveness and TNF-α mRNA expression in rat bronchi segments in E. coli lipopolysaccharide-induced airway inflammation by a NF-κB dependent mechanism, *Lasers Surg. Med*., 2009, **41**, 68–74.
49. MARTIN, R., Laser-accelerated inflammation/pain reduction and healing practical, *Pain Management*, 2003, Nov–Dec, 20–25.
50. MILLS, E.M., P.G. GUNASEKAR, G. PAVLAKOVIC, G.E. ISOM: Cyanide-induced apoptosis and oxidative stress in differentiated pc12 cells, *J. Neurochem*., 1996, **67**, 1039 –46.
51. MURAT, G., G. HURSIT OZER, O. BOZKULAK, H. OZGUR TABAKOGLU, E. AKTAS, G. DENIZ, C. ERTAN, The biological effects of 632.8 nm low energy He–Ne laser on peripheral blood mononuclear cells *in vitro*, *J. Photochem. Photobiol. B: Biology*, 2006, **82**(3), 199–202.
52. ORON, A., U. ORON, J. CHEN, A. EILAM, C. ZHANG, M. SADEH, Y. LAMPL, J. STREETER, L. DETABOADA, M. CHOPP, Low-level laser therapy applied transcranially to rats after induction of stroke significantly reduces long-term neurological deficits, *Stroke*, 2006, **37**, 2620–2624.
53. PAL, G., A. DUTTA, K. MITRA, M. S. GRACE, A. AMAT, T. B. ROMANCZYK, X. WU, K.CHAKRABARTI, J. ANDERS, E. GORMAN, R. W. WAYNANT, D. B. TATA, Effect of low intensity laser interaction with human skin fibroblast cells using fiber-optic nano-probes, *J. Photochem. Photobiol. B: Biology* , 2007, **86**, 252–261
54. POURZARANDIAN, A., H. WATANABE, S.M.P.M. RUWANPURA, A. AOKI, I. ISHIKAWA, Effect of low-level Er:YAG laser irradiation on cultured human gingival fibroblasts, *J. Periodont*., 2005, **76**, 187–193.
55. QADRI, T., P. BOHDANECKA, J. TUNÉR, L. MIRANDA, M. ALTAMASH, A. GUSTAFSSON The importance of coherence length in laser phototherapy of gingival inflammation: a pilot study, *Lasers Med. Sci.*, 2007, **22**(4), 245–251.
56. RIZZI, C.F., J.L. MAURIZ, D.S.F. CORREA, A.J. MOREIRA, C.G. ZETTLER, L.I. FILIPPIN, N.P. MARRONI, J. GONZALEZ-GALLEGO, Effects of low-level laser therapy (LLLT) on the nuclear factor (NF)-κB signaling pathway in traumatized muscle, *Lasers Surg. Med*., 2006, **38**, 704–713.
57. ROCHKIND, S, V. DRORY, M. ALON, M. NISSAN, G.E. OUAKNINE, Laser phototherapy (780 nm), a new modality in treatment of long-term incomplete peripheral nerve injury: a randomized double-blind placebo-controlled study, *Photomed. Laser Surg.*, 2007, **25**(5), 436–442.
58. SCHROEDER, P., C. POHL, C. CALLES, C. MARKS, S. WILD, J. KRUTMANN, Cellular response to infrared radiation involves retrograde mitochondrial signaling, *Free Radic. Biol. Med*., 2007, **43**, 128–135.
59. SEREMET, T., M. DUMITRESCU, S. RADESI, GY. KATONA, I.O. DOAGĂ, E. RADU, J. HORVÁTH, E. TANOS, L. KATONA, E. KATONA, Photobiomodulation of quercetin antiproliferative effects, seen in human acute T leukemic jurkat cells, *Rom. J. Biophys.*, 2007, **17**(1), 33–44.
60. SHEFER, G., I. BARASH, U. ORON, O. HALEVY, Low-energy laser irradiation enhances de novo protein synthesis via its effects on translation-regulatory proteins in skeletal muscle myoblasts, *Biochim. Biophys. Acta*, 2003, **1593**, 131–139.
61. SHEFER, G., T.A. PARTRIDGE, L. HESLOP, J.G. GROSS, U. ORON, O. HALEVY, Low energy laser irradiation promotes the survival and cell cycle entry of skeletal muscle satellite cells, *J. Cell Science*, 2002, **115**, 1461–1469.
62. SPLINTER, R., *An Introduction to Biomedical Optics*, CRC Press, Boca Raton, 2006.
63. TUBY, H., L. MALTZ, U. ORON, Low-level laser irradiation (LLLI) promotes proliferation of mesenchymal and cardiac stem cells in culture, *Lasers Surg. Med*., 2007, 39, 373–378.

64. TUNER, J., L. HODE, *Laser Therapy – Clinical Practice and Scientific Background*, Prima Books, Grängesberg, 2002.
65. WONG-RILEY, M.T., X. BAI, E. BUCHMAN, H.T. WHELAN: Light-emitting diode treatment reverses the effect of TTX on cytochrome c oxidase in neurons, *Neuroreport*, 2001, **12**, 3033–7.
66. WONG-RILEY, M.T.T., H.L. LIANG, J.T. EELLS, B. CHANCE, M.M. HENRY, E. BUCHAMANN, M. KANE, H.T.WHELAN, Photobiomodulatiom directly benefits primary neurons functionally inactivated by toxins, *J. Biol. Chem.*, 2005, **280**, 4761–71.
67. WOODRUFF, L., J. BOUNKEO, W. BRANNON, K. DAWES, C. BARHAM, D. WADDELL, C. ENWEMEKA, The efficacy of laser therapy in wound repair: a meta-analysis of the literature, *Photomed. Laser Surg*., 2004, **22**, 241–247.
68. ZHANG, Y., S. SONG, C.-C. FONG, C.-H. TSANG, Z. YANG, M. YANG, cDNA microarray analysis of gene expression proteins in human fibroblast cells irradiation with red light, *J. Invest. Dermatol.*, 2003, **120**, 849–857.